

Synthesis, crystal structures and magnetic properties of five new metal(II) compounds constructed with isomers of aminobenzonitrile and dicyanamide ligands

Moumita Biswas ^a, Georgina M. Rosair ^b, Guillaume Pilet ^c, M. Salah El Fallah ^{d,*},
Joan Ribas ^d, Samiran Mitra ^{a,*}

^a Department of Chemistry, Jadavpur University, Kolkata 700 032, West Bengal, India

^b Department of Chemistry, Heriot-Watt University, Edinburgh EH14 4AS, UK

^c Groupe de Cristallographie et Ingénierie Moléculaire, Laboratoire des Multimatériaux et Interfaces – UMR 5615 CNRS-Université Claude Bernard Lyon 1, Bât. Jules Raulin 43 Bd du 11 Novembre 1918, 69622 Villeurbanne Cedex, France

^d Department de Química Inorgànica, Universitat de Barcelona, Martí i Franquès, 1-11, 08028 Barcelona, Spain

Received 25 May 2006; accepted 2 August 2006

Available online 18 August 2006

Abstract

Five new compounds formulated as $[\text{Ni}^{\text{II}}(\text{dca})_2(\text{para-ABN})_2(\text{H}_2\text{O})_2]$ (**1**), $[\text{Cu}^{\text{II}}(\text{dca})_2(\text{para-ABN})_2(\text{H}_2\text{O})_2]$ (**2**), $[\text{Cu}^{\text{II}}(\text{dca})_2(\text{para-ABN})_2]_n$, (**3**), $[\text{Cu}^{\text{II}}(\text{dca})_2(\text{ortho-ABN})_2]_n$, (**4**) and $[\text{Cd}^{\text{II}}(\text{dca})_2(\text{meta-ABN})_2]_n$ (**5**), where dca = dicyanamide and ABN = aminobenzonitrile, have been synthesized and characterized by single crystal X-ray diffraction studies and low temperature (300–2 K) magnetic measurements. The structural analyses revealed that **1** and **2** are isomorphous where dca and *para*-ABN both act as monodentate ligands. **3** consists of infinite double stranded chains of Cu(II) ions connected through the *para*-ABN bridges whereas **4** and **5** consist of infinite double stranded chains of Cu(II) and Cd(II) respectively, connected through $\mu_{1,5}$ -dca bridges. The compounds extend their geometries to three-dimensional for **1–3** and **5** and two-dimensional for **4** through hydrogen bonding interactions. All the metal ions Ni^{2+} , Cu^{2+} and Cd^{2+} are located on inversion centres and have distorted octahedral coordination geometries. The variable temperature magnetic susceptibility measurements show that the global feature of the $\chi_{\text{M}}T$ versus T curves for **3** and **4** is characteristic of very weak antiferromagnetic interactions and between 300 and 2 K the best fit parameters were determined as $J = -2.35$ and -5.1 cm^{-1} , respectively.

© 2006 Elsevier Ltd. All rights reserved.

Keywords: Metal (nickel, copper, cadmium); Bridging ligands (dca, ABN); Supramolecular structures; Magnetic properties; First Cu–ABN compounds

1. Introduction

The bulk properties of a molecular material depend critically on its crystal structure and intermolecular interactions. Recently, enormous interests have been shown in coordination polymers, zeolitic structures, hydrogen-bonded networks and potentially important magnetic materials [1–3]. The main attractions for extended structures are

their tunability and potential applications [4–6]. There is also an aesthetic perspective; chemists are attracted by the particular beauty and the intriguing diversity of the structures, which can be obtained by assembling metal ions and various multifunctional ligands. The coordination geometry of the metal ion is crucial in the self-assembling process [7–11]. Solvent molecules and counter ions will also influence the final supramolecular architectures. These can affect the size, shape and hydrophilic character of voids in zeolitic structures and hydrogen-bonded networks as well as the overall stability of the supramolecular systems [5,7,12,13]. Our study describes two types of ligands namely

* Corresponding authors. Fax: +91 33 24146414 (S. Mitra).

E-mail addresses: salah.elfallah@qi.ub.es (M.S. El Fallah), smitra_2002@yahoo.com (S. Mitra).

dicyanamide (dca) and aminobenzonitrile (ABN) isomers for coordination with M(II) ions (M = Ni, Cu and Cd) in order to construct new and varied metal frameworks. The coordination polymers are formed when divalent first-row transition metals are linked with the generally bidentate (monodentate and tridentate coordination is also possible) dicyanamide (dca, $\text{N}(\text{CN})_2^-$) ligand. This ligand has significant current interest for their structural diversities and potentially interesting magnetic properties [14]. Aminobenzonitrile isomers can coordinate to a metal centre through either the amine or nitrile nitrogen. Accordingly, we have obtained five different structures where the above two ligands show different bonding modes to metal(II) ions.

In this paper, we report five compounds with the following formula $[\text{Ni}^{\text{II}}(\text{dca})_2(\text{para-ABN})_2(\text{H}_2\text{O})_2]$ (**1**), $[\text{Cu}^{\text{II}}(\text{dca})_2(\text{para-ABN})_2(\text{H}_2\text{O})_2]$ (**2**), $[\text{Cu}^{\text{II}}(\text{dca})_2(\text{para-ABN})_2]_n$ (**3**), $[\text{Cu}^{\text{II}}(\text{dca})_2(\text{ortho-ABN})_2]_n$ (**4**) and $[\text{Cd}^{\text{II}}(\text{dca})_2(\text{meta-ABN})_2]_n$ (**5**) using dicyanamido (dca) and three isomers of aminobenzonitrile (ABN) ligands. A CSD search [15,16] yielded only ten complex compounds with aminobenzonitriles. The present work contains the first coordination polymers of Cu(II) with ABN ligands. Two monomeric isomorphous compounds **1** and **2** and three polymeric frameworks **3–5** have been characterized. All except **4** (2D hydrogen bonding network) have an extensive 3D hydrogen bonding network.

2. Experimental

All reagents were of commercial grade and were used as received. $\text{Na}[\text{N}(\text{CN})_2]_2$, was purchased from the Aldrich Company.

2.1. Preparations

2.1.1. Synthesis of $[\text{Ni}(\text{dca})_2(\text{para-ABN})_2(\text{H}_2\text{O})_2]$ (**1**)

para-Aminobenzonitrile (0.0590 g, 0.5 mmol) was dissolved in 3 mL of methanol. The resultant solution was added to 3 mL of a methanolic solution of $\text{Ni}(\text{NO}_3)_2 \cdot 6\text{H}_2\text{O}$ (0.1454 g, 0.5 mmol). It was stirred for 1 h at room temperature. Then the mixture was placed in an ice-bath and the temperature maintained at 0 °C. Next, 5 mL aqueous solution of $\text{NaN}(\text{CN})_2$ (0.0445 g, 0.5 mmol) was added to the mixture. Green cubic crystals suitable for X-ray diffraction study were obtained from the mother liquor by slow evaporation at room temperature after 10 days. They were filtered off, washed with a small amount of water and dried in air. Elemental analysis: Calc. for $\text{NiC}_{18}\text{H}_{16}\text{N}_{10}\text{O}_2$: C 46.64, H 3.45, N 30.23%. Found: for **1** C 46.63, H 3.44, N 30.25%. Infrared spectrum: $[\text{N}(\text{CN})]^-$, $\nu_{\text{sym}}(\text{C}\equiv\text{N})$ 2195, $\nu_{\text{asym}}(\text{C}\equiv\text{N})$ 2237, $\nu_{\text{sym}}(\text{C}-\text{N})$ 922 and $\nu_{\text{asym}}(\text{C}-\text{N})$ 1370; ABN, $\nu(\text{N}-\text{H})$ 3444 cm^{-1} .

2.1.2. Synthesis of $[\text{Cu}(\text{dca})_2(\text{para-ABN})_2(\text{H}_2\text{O})_2]$ (**2**)

The preparation of **2** was the same as stated for compound **1**, using $\text{Cu}(\text{NO}_3)_2 \cdot 3\text{H}_2\text{O}$ (0.1208 g, 0.5 mmol) instead of $\text{Ni}(\text{NO}_3)_2 \cdot 6\text{H}_2\text{O}$. Dark green crystals suitable

for X-ray diffraction were formed after 10 days. They were filtered off, washed with a small amount of water and dried in air. Elemental analysis: Calc. for $\text{CuC}_{18}\text{H}_{16}\text{N}_{10}\text{O}_2$: C 46.16, H 3.42, N 29.92%. Found: for **2** C 46.14, H 3.41, N 29.94%. Infrared spectrum: $[\text{N}(\text{CN})]^-$, $\nu_{\text{sym}}(\text{C}\equiv\text{N})$ 2195, $\nu_{\text{asym}}(\text{C}\equiv\text{N})$ 2227, $\nu_{\text{sym}}(\text{C}-\text{N})$ 915 and $\nu_{\text{asym}}(\text{C}-\text{N})$ 1345; ABN, $\nu(\text{N}-\text{H})$ 3443 cm^{-1} .

2.1.3. Synthesis of $[\text{Cu}(\text{dca})_2(\text{para-ABN})_2]_n$ (**3**)

para-Aminobenzonitrile (0.0590 g, 0.5 mmol) was dissolved in 5 mL of methanol. The resultant solution was added to 5 mL of a methanolic solution of $\text{Cu}(\text{NO}_3)_2 \cdot 3\text{H}_2\text{O}$ (0.1208 g, 0.5 mmol). The mixture was heated under reflux for half an hour at 45–50 °C after which it was cooled and to it 3 mL aqueous solution of $\text{NaN}(\text{CN})_2$ (0.0445 g, 0.5 mmol) was added and the resultant solution was stirred for 1 h at room temperature. It was filtered off and the filtrate was kept at room temperature. Green cubic crystals suitable for X-ray diffraction study were obtained after two weeks. They were filtered off, washed with a small amount of water and dried in air. Yield 68%. Elemental analysis: Calc. for $\text{CuC}_{18}\text{H}_{12}\text{N}_{10}$: C 50.01, H 2.78, N 32.41%. Found: for **3**: C 50.02, H 2.77, N 32.39%. Infrared spectrum: $[\text{N}(\text{CN})]^-$, $\nu_{\text{sym}}(\text{C}\equiv\text{N})$ 2190, $\nu_{\text{asym}}(\text{C}\equiv\text{N})$ 2235, $\nu_{\text{sym}}(\text{C}-\text{N})$ 935 and $\nu_{\text{asym}}(\text{C}-\text{N})$ 1357; ABN, $\nu(\text{N}-\text{H})$ 3440 cm^{-1} .

2.1.4. Synthesis of $[\text{Cu}(\text{dca})_2(\text{ortho-ABN})_2]_n$ (**4**)

This compound was synthesized as for **3** but from $\text{Cu}(\text{NO}_3)_2 \cdot 3\text{H}_2\text{O}$ (0.1208 g, 0.5 mmol) and *ortho*-aminobenzonitrile (0.0590 g, 0.5 mmol). Green cubic crystals suitable for X-ray diffraction study were obtained from the mother liquor by slow evaporation at room temperature after 7 days. They were filtered off, washed with a small amount of water and dried in air. Yield 65%. Elemental analysis: Calc. for $\text{CuC}_{18}\text{H}_{12}\text{N}_{10}$: C 50.01, H 2.78, N 32.41%. Found: for **4**: C 50.03, H 2.79, N 32.38%. Infrared spectrum: $[\text{N}(\text{CN})]^-$, $\nu_{\text{sym}}(\text{C}\equiv\text{N})$ 2186, $\nu_{\text{asym}}(\text{C}\equiv\text{N})$ 2230, $\nu_{\text{sym}}(\text{C}-\text{N})$ 900 and $\nu_{\text{asym}}(\text{C}-\text{N})$ 1371; ABN, $\nu(\text{N}-\text{H})$ 3440 cm^{-1} .

2.1.5. Synthesis of $[\text{Cd}(\text{dca})_2(\text{meta-ABN})_2]_n$ (**5**)

This compound was synthesized as for **3** but from $\text{Cd}(\text{NO}_3)_2 \cdot 4\text{H}_2\text{O}$ (0.1542 g, 0.5 mmol) and *meta*-aminobenzonitrile (0.0590 g, 0.5 mmol). Colourless crystals were formed after 3–4 weeks. They were filtered off, washed with small amount of water and dried in air. Yield 66%. Elemental analysis: Calc. for $\text{CdC}_{18}\text{H}_{12}\text{N}_{10}$: C 44.93, H 2.50, N 29.12%. Found: for **5**: C 44.90, H 2.49, N 29.14%. Infrared spectrum: $[\text{N}(\text{CN})]^-$, $\nu_{\text{sym}}(\text{C}\equiv\text{N})$ 2185, $\nu_{\text{asym}}(\text{C}\equiv\text{N})$ 2230, $\nu_{\text{sym}}(\text{C}-\text{N})$ 905 and $\nu_{\text{asym}}(\text{C}-\text{N})$ 1355; ABN, $\nu(\text{N}-\text{H})$ 3440 cm^{-1} .

2.2. Physical measurements

The elemental analyses (C, H, N) were carried out with a Perkin Elmer 2400 II elemental analyser. For each sample

the analyses were carried out in duplicate. The FT-IR spectra were recorded on Perkin Elmer RX I FT-IR spectrophotometer from KBr pellets in range 4000–400 cm^{-1} . It is important for the characteristic bands of the dca ligand and amino group.

Magnetic susceptibility measurements for **3** and **4** were carried out on polycrystalline samples, with a Quantum Design SQUID MPMS-XL susceptometer apparatus working in the range 2–300 K under a magnetic field of approximately 500 G (2–30 K) and 10000 G (35–300 K). Diamagnetic corrections were estimated from Pascal tables.

2.3. Crystal data collection and refinement

Single crystal diffraction data for **1–3** and **5** were collected on a Bruker Nonius X8 Apex 2 CCD diffractometer at 100 K, cooled by an Oxford Cryosystems Cryostream. The crystals were covered in Paratone-N oil and mounted in cryoloops. The structures were solved and refined using the SHELXTL [17] suite of programs. Amine and water H atoms were located in the difference Fourier map and isotropic displacement parameters were freely refined for **1** and **5**, and riding for **3** and **2**. The data for **4** were collected on a Nonius KappaCCD diffractometer; [18] the lattice constants were refined by least-square refinement using 2005 reflections ($2.1^\circ < \theta < 27.8^\circ$). No absorption correction was applied to the data sets. The structure was solved by direct methods [19] and refined [20] against F using reflections with $[I/\sigma(I) > 3]$. All non-hydrogen atoms were successfully refined with anisotropic displacement factors. Further experimental details for all the compounds are summarized in Table 1.

3. Results and discussion

In the five compounds, both dca and ABN ligands show varied bonding modes, i.e. (i) dca acts as bridging ligand for **4** and **5**, (ii) *para*-ABN acts as bridging ligand for **3** and (iii) both the dca and *para*-ABN ligands act as monodentate ligands for **1** and **2**. *ortho*- and *meta*-ABN act as monodentate ligands in **4** and **5**, respectively. These resulted in four generally different structural frameworks. The formation of compounds **2** and **3** was highly dependent on the reaction conditions. In both cases the starting materials were used in the same ratio, $\text{Cu}(\text{NO}_3)_2$:dca:*para*-ABN of 1:1:1, but the different synthetic methods employed yielded two new compounds. In the synthesis of **3** when an aqueous solution of $\text{NaN}(\text{CN})_2$ was added to a methanolic solution of $\text{Cu}(\text{NO}_3)_2$ and *para*-aminobenzonitrile, a deep-green precipitate was formed within a few minutes, during the stirring. On filtration a green coloured solution was obtained which on keeping yielded **3**. The deep-green precipitate was characterized by IR and X-ray powder diffraction study and the found results were identical with those of **2**. From this it was concluded that **3** was the major and thermodynamically controlled product, whereas **2** was the minor and kinetically controlled product in the preparative process of **3**. The low temperature preparative process produced **2** exclusively.

3.1. Crystal structure analyses

Crystal structure analyses show that **1** and **2** are monomeric compounds and form two-dimensional hydrogen bonded sheets through the interaction of the *para*-ABN and dicyanamide ligands which further extend

Table 1
Experimental parameters for the crystal structure analyses

Compound	1	2	3	4	5
Empirical formula	$\text{NiC}_{18}\text{H}_{16}\text{N}_{10}\text{O}_2$	$\text{CuC}_{18}\text{H}_{16}\text{N}_{10}\text{O}_2$	$\text{CuC}_{18}\text{H}_{12}\text{N}_{10}$	$\text{CuC}_{18}\text{H}_{24}\text{N}_{20}$	$\text{CdC}_{18}\text{H}_{12}\text{N}_{10}$
Formula weight	463.12	467.95	431.92	431.91	480.78
Temperature (K)	100(2)	100(2)	100(2)	293	100(2)
Crystal system	triclinic	triclinic	triclinic	triclinic	monoclinic
Space group	$P\bar{1}$	$P\bar{1}$	$P\bar{1}$	$P\bar{1}$	$P2_1/n$
a (Å)	7.1952(6)	7.2159(19)	7.2105(8)	7.1128(2)	7.7055(15)
b (Å)	7.6033(7)	7.600(2)	7.9475(9)	7.1730(4)	8.7676(17)
c (Å)	9.8968(9)	9.897(3)	9.4240(10)	9.8358(6)	13.806(3)
α (°)	104.674(3)	104.713(7)	99.740(4)	89.511(3)	90
β (°)	92.945(3)	92.879(7)	110.095(4)	85.069(3)	90.262(4)
γ (°)	101.929(3)	102.055(7)	109.258(4)	71.300(3)	90
Volume (Å ³)	509.37(8)	510.3(2)	453.83(9)	473.48(4)	932.7(3)
Z	1	1	1	1	2
D_c (Mg m^{-3})	1.510	1.523	1.580	1.515	1.712
μ (mm^{-1})	0.991	1.109	1.232	1.181	1.199
Reflections collected	10555	6903	14525	3405	23446
Independent reflections $[R_{\text{int}}]$	3613 [0.0213]	3509 [0.0222]	3278 [0.0324]	2214 [0.0270]	2987 [0.0363]
Data/restraints/parameters	3613/0/158	3509/2/154	3278/0/139	1289/0/133	2987/0/141
R_1 [$I > 2\sigma(I)$]	0.0242	0.0394	0.0332	0.0411	0.0266
R_1 (all data)	0.0258	0.0450	0.0408	0.0940	0.0363
wR_2 [$I > 2\sigma(I)$]	0.0741	0.1142	0.0864	0.0476	0.0712
wR_2 (all data)	0.0749	0.1168	0.0885	0.0886	0.0727

the structures to three dimensions through weak π - π interactions from the aromatic group of *para*-ABN ligands. **3–5** revealed that one-dimensional double stranded polymeric chains were formed. These infinite chains were further connected via hydrogen bonding interactions to extend the network into 3D in **3** and **5** and 2D in **4**

Self-association has taken place in a variety of ways. Firstly intermolecular interactions have been propagated solely through ligand $\text{OH}\cdots\text{N}$ and $\text{NH}\cdots\text{N}$ hydrogen bonds (in **1** and **2**), secondly through two *trans*-coordinated dca ligands and two *cis* amine bonded *para*-ABN ligands (in **3**) and thirdly by *trans*-coordinated amine groups of two ABN and two *cis* dca ligands (in **4** and **5**). Selected bond lengths and angles for **1–5** are given in Tables 2–6, respectively. The compounds have an extensive 3D (**1–3** and **5**) or 2D (**4**) hydrogen bonding networks; these details are summarized in Table 7.

The structures of $[\text{Ni}(\text{dca})_2(\text{para-ABN})_2(\text{H}_2\text{O})_2]$ (**1**) and $[\text{Cu}(\text{dca})_2(\text{para-ABN})_2(\text{H}_2\text{O})_2]$ (**2**) are virtually identical and are exemplified by **1**. The crystal structure of **1** consists of centrosymmetric, mononuclear $[\text{Ni}(\text{dca})_2(\text{para-ABN})_2-$

$(\text{H}_2\text{O})_2]$ entities. Both *para*-ABN and dicyanamide act as terminal ligands (Figs. 1 and 2). The *para*-ABN ligand is coordinated to the metal ion through the amine nitrogen atom. The Ni–N bond lengths are Ni–N(dca) = 2.0351 Å and Ni–N(*para*-ABN) = 2.1513 Å. The two Ni–O (aqua) distances are 2.0700 Å. The nickel(II) ion exhibits a *trans* distorted octahedral stereochemistry. The C–N–C angle of the dicyanamide is 120.91°. The most intriguing features of the crystal structure of the compound arise from interactions at the supramolecular level. The *para*-ABN ligand acts as both a hydrogen donor (through the amine group) and a hydrogen acceptor (through the nitrile group) while the dicyanamide ligand acts as a hydrogen acceptor and the aqueous ligand acts as a hydrogen donor. The hydrogen bonding network for both **1** and **2** consists of layers. Each layer consists of interlocked parallelograms. One set of parallel sides is doubly-bridging *para*-ABN and the other doubly-bridging dca. In the latter, the bridge is formed between dca and *para*-ABN rather than with the metal ion. This supramolecular architecture is shown in Fig. 3. The interlayer interactions are of a weak π - π nature

Table 2
Selected interatomic distances (Å) and angles (°) for **1**

Ni(1)–N(11)	2.0351(8)	Ni(1)–O(1)	2.0700(7)
Ni(1)–N(1)	2.1513(8)	N(1)–C(2)	1.4169(11)
N(1)–H(11N)	0.898(15)	N(1)–H(12N)	0.881(16)
O(1)–H(11W)	0.787(19)	O(1)–H(12W)	0.757(19)
C(8)–N(9)	1.1484(14)	C(11)–N(11)	1.1549(12)
C(11)–N(12)	1.3097(12)	C(12)–N(13)	1.1576(13)
C(12)–N(12)	1.3084(13)		
N(11)–Ni(1)–O(1)	89.14(3)	N(11)–Ni(1)–O(1)#1	90.86(3)
O(1)–Ni(1)–O(1)#1	180.0	N(11)–Ni(1)–N(1)	85.00(3)
O(1)–Ni(1)–N(1)	91.97(3)	O(1)#1–Ni(1)–N(1)	88.03(3)
N(11)–Ni(1)–N(1)#1	95.00(3)	C(2)–N(1)–Ni(1)	117.58(6)
C(2)–N(1)–H(11N)	111.2(9)	Ni(1)–N(1)–H(11N)	102.7(10)
C(2)–N(1)–H(12N)	108.1(10)	Ni(1)–N(1)–H(12N)	104.9(11)
H(11N)–N(1)–H(12N)	112.3(15)	Ni(1)–O(1)–H(11W)	110.6(12)
Ni(1)–O(1)–H(12W)	118.5(14)	H(11W)–O(1)–H(12W)	104.6(18)
C(12)–N(12)–C(11)	120.73(9)		

Symmetry transformations used to generate equivalent atoms: #1 $-x, -y + 2, -z + 2$.

Table 3
Selected interatomic distances (Å) and angles (°) for **2**

Cu(1)–N(11)	2.0318(15)	Cu(1)–O(1)	2.0748(12)
Cu(1)–N(1)	2.1481(14)	N(1)–C(2)	1.416(2)
N(1)–H(11N)	0.80(2)	N(1)–H(12N)	0.84(2)
O(1)–H(11W)	0.730(16)	O(1)–H(12W)	0.709(16)
C(8)–N(9)	1.147(2)	N(11)–C(12)	1.154(2)
C(12)–N(12)	1.307(2)	N(12)–C(13)	1.307(2)
C(13)–N(13)	1.158(2)		
N(11)#1–Cu(1)–O(1)	90.97(5)	N(11)–Cu(1)–O(1)	89.03(5)
O(1)–Cu(1)–O(1)#1	180.0	N(11)#1–Cu(1)–N(1)	94.84(5)
N(11)–Cu(1)–N(1)	85.16(6)	O(1)–Cu(1)–N(1)	92.09(5)
O(1)#1–Cu(1)–N(1)	87.91(5)	C(2)–N(1)–Cu(1)	117.86(10)
Cu(1)–N(1)–H(11N)	103.8(17)	Cu(1)–N(1)–H(12N)	106.2(16)
Cu(1)–O(1)–H(11W)	107.1(19)	Cu(1)–O(1)–H(12W)	121(2)
H(11W)–O(1)–H(12W)	107(3)	N(9)–C(8)–C(5)	177.68(19)
C(12)–N(12)–C(13)	120.91(14)		

Symmetry transformations used to generate equivalent atoms: #1 $-x + 2, -y + 1, -z + 1$.

Table 4
Selected interatomic distances (Å) and angles (°) for **3**

Cu(1)–N(1)	2.0550(12)	Cu(1)–N(11)	1.9763(12)
Cu(1)–N(9)	2.497	N(1)–C(2)	1.4284(16)
N(1)–H(12N)	0.798(19)	C(2)–C(3)	1.3951(18)
C(2)–C(7)	1.3955(19)	C(3)–C(4)	1.3884(18)
C(3)–H(3)	0.9500	C(4)–C(5)	1.402(2)
C(4)–H(4)	0.9500	C(5)–C(6)	1.3932(19)
C(5)–C(8)	1.4453(18)	C(6)–C(7)	1.3893(18)
N(1)–H(11N)	0.780(18)		
N(11)–Cu(1)–N(11)#1	180.00(9)	N(11)–Cu(1)–N(1)#1	90.78(5)
N(11)#1–Cu(1)–N(1)#1	89.22(5)	N(11)–Cu(1)–N(1)	89.22(5)
N(11)#1–Cu(1)–N(1)	90.78(5)	N(1)#1–Cu(1)–N(1)	180.00(6)
C(2)–N(1)–Cu(1)	114.34(8)	C(2)–N(1)–H(11N)	111.2(13)
Cu(1)–N(1)–H(11N)	104.9(13)	C(2)–N(1)–H(12N)	114.9(13)
Cu(1)–N(1)–H(12N)	103.0(13)	H(11N)–N(1)–H(12N)	107.5(18)
C(3)–C(2)–C(7)	120.33(12)	C(3)–C(2)–N(1)	119.25(12)
C(7)–C(2)–N(1)	120.29(12)	C(4)–C(3)–C(2)	120.15(12)
C(4)–C(3)–H(3)	119.9	C(11)–N(12)–C(12)	118.35(12)

Symmetry transformations used to generate equivalent atoms: #1 $-x, -y, -z$.

Table 5
Selected interatomic distances (Å) and angles (°) for **4**

Cu(1)–N(1)	1.965(3)	Cu(1)–N(5)	1.989(3)
Cu(1)–N(11)	2.564(3)	N(11)–C(12)	1.396(5)
C(12)–C(13)	1.390(5)	C(13)–C(14)	1.386(6)
C(14)–C(15)	1.384(7)	C(15)–C(16)	1.361(6)
C(16)–C(17)	1.400(6)	C(17)–C(12)	1.401(5)
C(17)–C(18)	1.437(5)	C(18)–N(19)	1.147(5)
N(1)–C(2)	1.141(4)	C(2)–N(3)	1.299(4)
N(3)–C(4)	1.291(4)	C(4)–N(5)	1.149(4)
N(1)–Cu(1)–N(1)	179.994	N(1)–Cu(1)–N(5)	91.4(1)
N(1)–Cu(1)–N(5)	88.6(1)	N(5)–Cu(1)–N(5)	179.994
N(1)–Cu(1)–N(11)	89.4(1)	N(1)–Cu(1)–N(11)	90.6(1)
N(5)–Cu(1)–N(11)	93.0(1)	N(5)–Cu(1)–N(11)	87.0(1)
N(11)–Cu(1)–N(11)	179.996		

between the *para*-ABN aromatic rings which results in the third dimensions and in **1** and **2** the centroid–centroid distances are 3.8159(7) and 3.8141(15) Å, respectively.

Table 6
Selected interatomic distances (Å) and angles (°) for **5**

Cd(1)–N(2)	2.3259(15)	Cd(1)–N(11)	2.3326(15)
Cd(1)–N(1)	2.3737(15)	N(1)–C(1)	1.423(2)
N(1)–H(1N)	0.99(2)	N(1)–H(2N)	0.87(2)
N(11)–C(12)	1.162(2)	C(12)–N(13)	1.312(2)
N(13)–C(20)#2	1.302(2)	N(2)–C(20)	1.149(2)
C(20)–N(13)#3	1.301(2)		
N(2)–Cd(1)–N(11)	95.16(5)	N(2)#1–Cd(1)–N(11)	84.84(5)
N(2)–Cd(1)–N(1)#1	87.32(5)	N(11)–Cd(1)–N(1)#1	93.11(5)
N(2)–Cd(1)–N(1)	92.68(5)	N(11)–Cd(1)–N(1)	86.89(5)
N(1)#1–Cd(1)–N(1)	180.00(6)	C(1)–N(1)–Cd(1)	116.11(10)
C(1)–N(1)–H(1N)	108.2(13)	Cd(1)–N(1)–H(1N)	105.4(13)
C(1)–N(1)–H(2N)	109.0(14)	Cd(1)–N(1)–H(2N)	109.3(16)
H(1N)–N(1)–H(2N)	108.7(19)	N(7)–C(7)–C(5)	179.07(19)
C(12)–N(11)–Cd(1)	155.06(14)	C(20)#2–N(13)–C(12)	120.04(15)
C(20)–N(2)–Cd(1)	152.80(13)		

Symmetry transformations used to generate equivalent atoms: #1 $-x + 1, -y + 1, -z$; #2 $x + 1, y, z$; #3 $x - 1, y, z$.

Table 7
Hydrogen-bonding parameters

Compound	D–H...A	$d(\text{D–H})$	$d(\text{H...A})$	$d(\text{D...A})$	(D–H...A)
1	N(1)–H(11N)...N(13)#5	0.898(15)	2.182(15)	3.0539(12)	163.8(13)
	O(1)–H(11W)...N(13)#5	0.787(19)	2.067(19)	2.8332(12)	164.4(17)
	N(1)–H(12N)...N(12)#6	0.881(16)	2.307(17)	3.1772(13)	169.7(15)
	O(1)–H(12W)...N(9)#7	0.757(19)	2.116(19)	2.8652(12)	170.7(18)
2	N(1)–H(11N)...N(13)#8	0.80(2)	2.28(2)	3.064(2)	164(2)
	N(1)–H(12N)...N(12)#9	0.84(2)	2.36(2)	3.185(2)	170(2)
	O(1)–H(11W)...N(13)#10	0.730(16)	2.112(17)	2.832(2)	169(3)
	O(1)–H(12W)...N(9)#4	0.709(16)	2.170(17)	2.862(2)	166(3)
3	N(1)–H(11N)...N(12)#1	0.780(18)	2.319(19)	3.0984(17)	176.7(17)
	N(1)–H(12N)...N(13)#2	0.798(19)	2.198(19)	2.9905(17)	171.8(17)
4	N(11)–H(5)...N(19)	0.91	2.42	3.257(5)	154
5	N(1)–H(1N)...N(13)#3	0.99(2)	2.81(2)	3.471(2)	125.0(16)
	N(1)–H(2N)...N(7)#4	0.87(2)	2.32(2)	3.121(2)	153(2)

Symmetry operator codes: #1 $-x + 1, -y, -z$; #2 $x - 1, y - 1, z$; #3 $-x + 3/2, y + 1/2, -z + 1/2$; #4 $-x + 1/2, y + 1/2, -z + 1/2$; #5 $-x + 1, -y + 3, -z + 2$; #6 $-x, -y + 3, -z + 2$; #7 $-x, -y + 1, -z + 1$; #8 $-x + 3, -y + 2, -z + 1$; #9 $-x + 2, -y + 2, -z + 1$; #10 $-x + 2, -y, -z$.

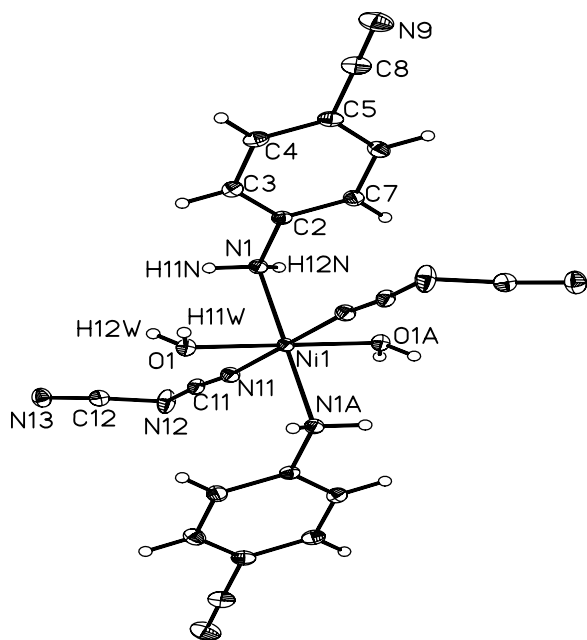


Fig. 1. Ortep view of **1** with the atom numbering scheme.

Fig. 4 shows a perspective view of **3** which is found to be a $[\text{Cu}(\text{dca})_2(\text{para-ABN})_2]$ asymmetric unit. This unit contains two terminal dicyanamido ligands and four bridging *para-ABN* ligands which adopt a distorted octahedral coordination sphere. The terminal dca ligands coordinate through the nitrile N(11) atoms, occupying the axial positions with $\text{Cu}(1)\text{--N}(11)$ 1.9763(12) Å, while the equatorial plane contains four nitrogen atoms from bridging *para-ABN* ligands which coordinate through the two amino N(1) atoms and two nitrile N(9) atoms [$\text{Cu}(1)\text{--N}(1)$ 2.0550(12) and $\text{Cu}(1)\text{--N}(9)$ 2.497 Å]. The $[\text{Cu}(\text{dca})_2-$

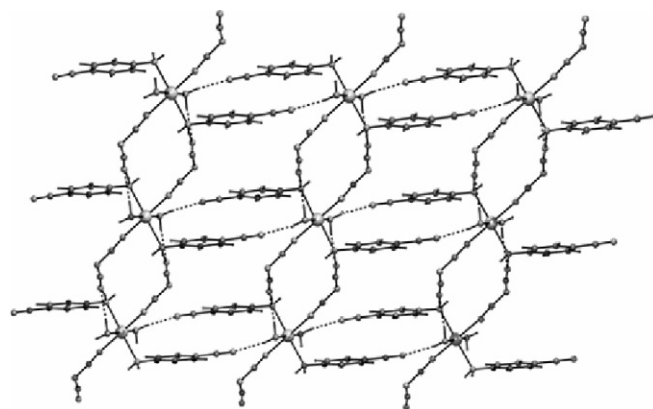


Fig. 3. Packing diagram of **1** with hydrogen bonding shown as a dotted line.

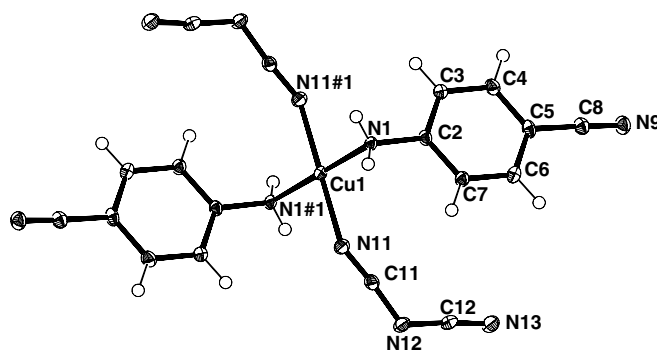


Fig. 4. Ortep view of **3** showing the atom numbering scheme.

(*para-ABN*)₂] monomer units are linked through bridging *para-ABN* ligands to make a double stranded polymeric chain (Fig. 5). The coordination polymer runs parallel to

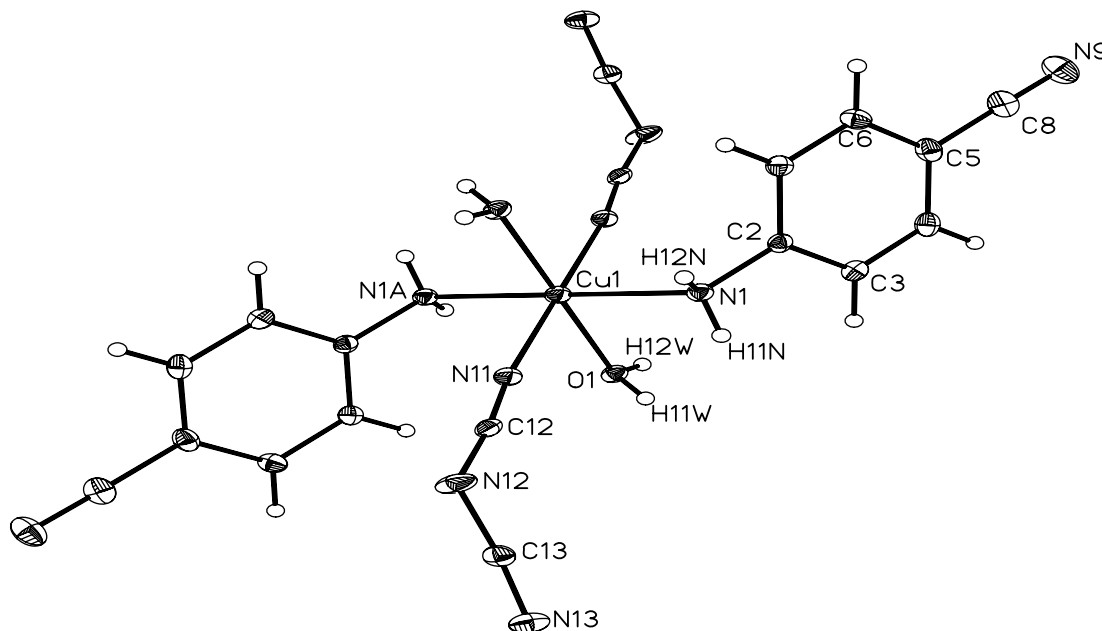


Fig. 2. Ortep view of **2** with the atom numbering scheme.

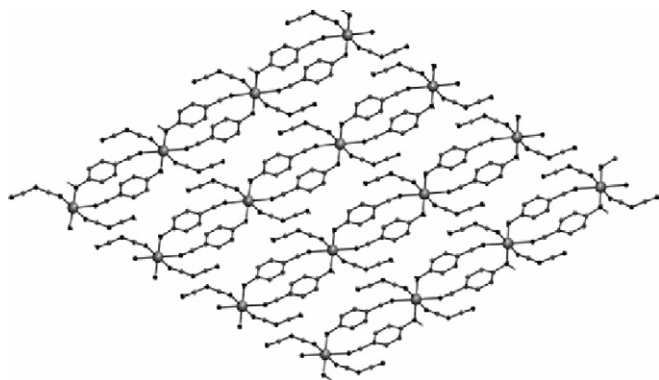


Fig. 5. Packing diagram of **3** omitting the H-bonding for clarity.

the crystallographic *a*-axis (Fig. 5), which is also observed for compounds **4** and **5**. The metal–metal distance between adjacent Cu centres within one polymer strand is equal to 9.7020 Å, while the closest Cu···Cu distance between two neighbouring strands is 8.795 Å.

Compound **3** shows a rarely observed characteristic, namely doubly bridging of the *para*-ABN ligand which binds via both the amine and nitrile nitrogen atoms. Dicyanamide can also be considered as a doubly bridging ligand but the bridge is made by a NH···N hydrogen bond to a *para*-ABN amine, which extends the geometry into three dimensions (Supporting information 1). The cobalt and nickel thiocyanate complexes [11] also have double bridging ABN ligands and the SCN ligands remain terminally bound but are involved in NH···S hydrogen bonds.

In **4** (Fig. 6) the *dca* ligands form bridges and the *ortho*-ABN ligands are terminal in contrast to the coordination mode of *dca* and *para*-ABN ligands in **3**. The copper(II)

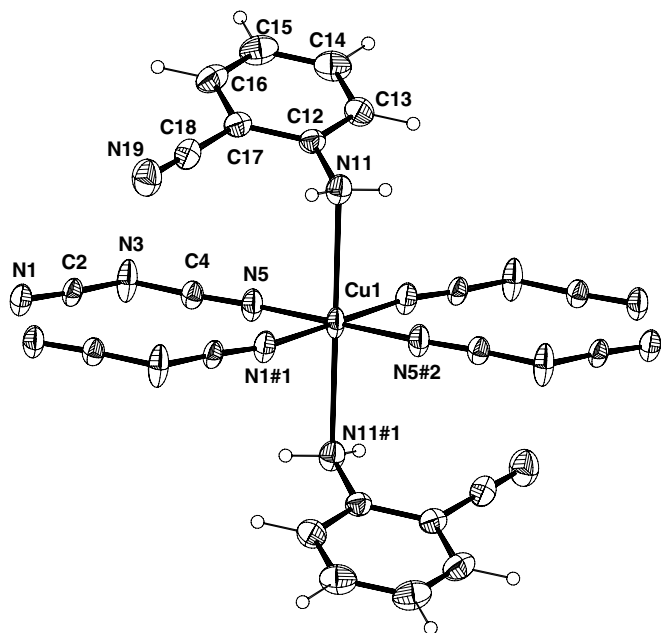


Fig. 6. ORTEP view of **4** with the atom numbering scheme.

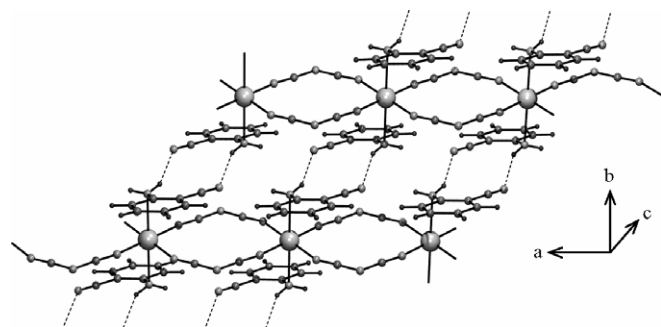


Fig. 7. View of the propagation of **4**.

ion coordination sphere is formed by two *dca* ligands bridging the pairs of Cu atoms while the amino groups from *ortho*-ABN ligands coordinate in the axial positions (Fig. 7). The metal–metal distance between adjacent Cu centres within one polymer strand is equal to 7.113 Å, while the closest Cu···Cu distance between two neighbouring strands is 7.173 Å. The NH···N hydrogen bond between two neighbouring polymer strands extend the structure of **4** into two-dimensions with the amine group from the *ortho*-ABN ligand acting as a hydrogen donor and nitrile group from the same ligand of another strand acting as a hydrogen acceptor (Fig. 7).

The structure of **5** (Fig. 8) is very similar to that of **4** and it is worthwhile to note that the metal–metal distance between adjacent Cd centres within the polymer strand is 7.705 Å, whilst the closest Cd···Cd distance between two neighbouring strands is 8.768 Å. The non-bridging *meta*-ABN ligands are bound to Cd with the amine group. They are orientated anti to each other with the torsion angle C(7A)–N(7A)–N(7)–C(7) being 180° as the Cd atom lies on an inversion centre.

The polymer strands of **3** and **5** are interconnected in three dimensions by an extensive network of NH···N hydrogen bonds. In **3** the amine group from the *para*-ABN ligand acts as the hydrogen donor and both nitrile and amide nitrogen atoms from dicyanamide ligands of another strand act as hydrogen acceptors (Fig. 5). While in **5** the amine group from *meta*-ABN acts as the hydrogen donor and the nitrogen atoms of the nitrile group from

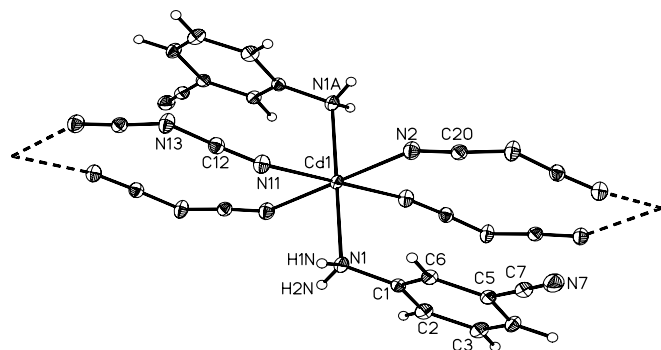


Fig. 8. ORTEP view of **5** with the atom numbering scheme.

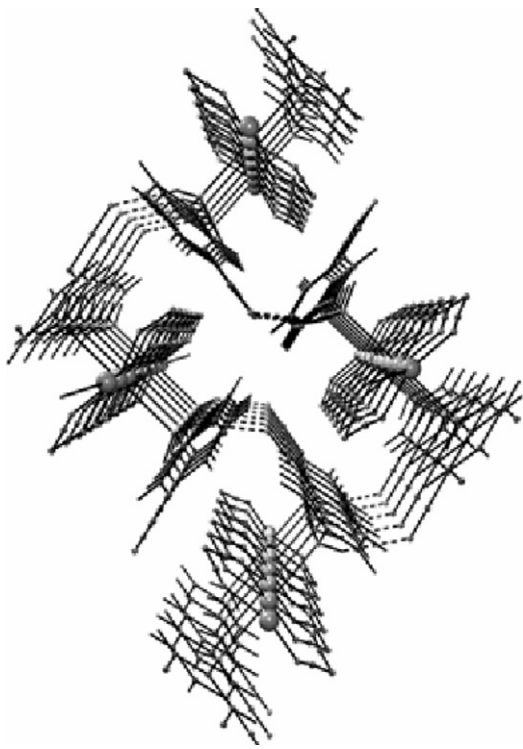


Fig. 9. Packing diagram of **5** with hydrogen bonding shown as a dotted line.

both *meta*-ABN and dicyanamide ligands of another strand act as hydrogen acceptors (Fig. 9). Although **4** and **5** show very similar connectivity, **4** has a hydrogen bonding network which extends into two dimensions and **5** extends into three dimensions. The position of the nitrile group of the ABN ligands for **4** and **5** is different i.e. *ortho*-ABN and *meta*-ABN respectively, so the *meta*-ABN isomer may be more able to form hydrogen-bonds compared to the *ortho*-ABN isomer, possibly for steric reasons.

3.2. Magnetochemistry

Variable temperature magnetic susceptibility measurements have been performed for **3** and **4**. The global feature of the $\chi_M T$ versus T curves in both compounds is characteristic of very weak antiferromagnetic interactions (Figs. 10 and 11). For **3** the value of $\chi_M T$ at 300 K is $0.384 \text{ cm}^3 \text{ K mol}^{-1}$ which is as expected for one uncoupled copper(II) ion ($0.37 \text{ cm}^3 \text{ K mol}^{-1}$ per Cu(II) with $g = 2.0$). With decreasing temperature, the $\chi_M T$ value remains almost constant until ca. 70 K and then it decreases sharply, giving the minimum value of $0.170 \text{ cm}^3 \text{ K mol}^{-1}$ at 2 K. The drop in $\chi_M T$ at low temperatures indicates the presence of a very weak antiferromagnetic coupling between the copper(II) ions.

As is shown in Fig. 5, the structure of **3** consists of copper entities linked by two *para*-ABN ligands, which also acts as hydrogen donors via the amine groups, and both nitrile and amide nitrogen atoms of dicyanamide act as hydrogen acceptors to give a 3D compound. To interpret

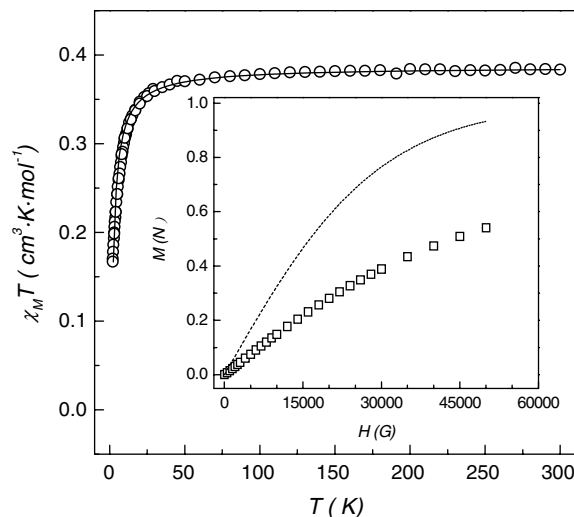


Fig. 10. Plot of $\chi_M T$ vs. T and $M(N_\beta)$ vs. $H(G)$ (inset) for **3**.

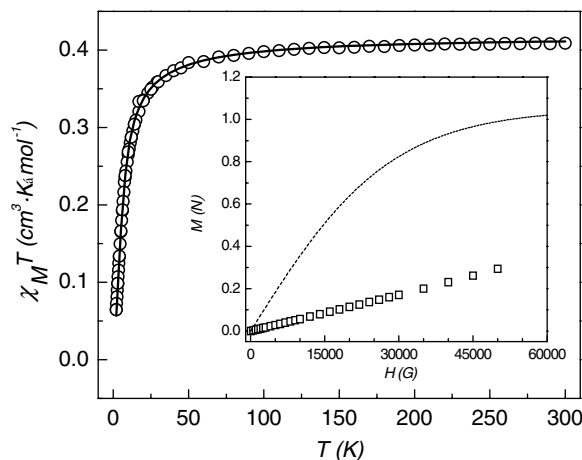


Fig. 11. Plot of $\chi_M T$ vs. T and $M(N_\beta)$ vs. $H(G)$ (inset) for **4**.

the magnetic behaviour of **3** we assume a negligible contribution from the interactions through the hydrogen bonding. The system may be treated in a simplified form as a uniform chain of Cu(II) atoms. Thus, only one coupling parameter (J) must be considered to interpret a possible magnetic interaction. The experimental magnetic data have been fitted using the equation, derived from the Bonner–Fisher [21] calculation based on the isotropic Heisenberg Hamiltonian: $H = -J \sum (S_i S_{i+1})$. The best fit parameters from 300 down to 2 K are found as $J = -2.35 \text{ cm}^{-1}$ and $g = 2.03$ with an error $R = 3.2 \times 10^{-5}$, where $R = \sum [(\chi_M T)_{\text{exp}} - (\chi_M T)_{\text{calc}}]^2 / \sum [(\chi_M T)_{\text{exp}}]^2$. The very low value of the superexchange parameter can be understood considering the large Cu...Cu distance (9.702 Å). The weak antiferromagnetic interaction was confirmed by magnetization measurements at 2 K up to an external field of 5 T. At higher field, the magnetization in $M/N\beta$ units indicates a value of 0.54; (a quasi half saturated $S = 1/2$ system) (inset Fig. 10). Comparison of the overall shape

of the plot with the Brillouin plot (dashed plot) for one isolated ion with $S = 1/2$ system and $g = 2$ indicates slower magnetization which is consistent with a weak antiferromagnetic interaction.

For **4** the value of $\chi_M T$ at 300 K is $0.409 \text{ cm}^3 \text{ mol}^{-1} \text{ K}$ which is as expected for one uncoupled copper(II) ion ($0.413 \text{ cm}^3 \text{ mol}^{-1} \text{ K}$ per one Cu^{II} with $g = 2.1$). The $\chi_M T$ values are constant over the temperature range, decreasing to $0.0644 \text{ cm}^3 \text{ mol}^{-1} \text{ K}$, at very low temperatures (2 K). The χ_M curve starts at $1.36 \times 10^{-3} \text{ cm}^3 \text{ mol}^{-1}$ at room temperature and increases in a uniform way to $0.0322 \text{ cm}^3 \text{ mol}^{-1}$ at 2 K. The weak antiferromagnetic interaction was confirmed by magnetization measurements at 2 K up to an external field of 5 T. At higher field, the magnetization in $M/N\beta$ units indicates a 0.2945 value for **4** (inset Fig. 11). Comparison of the overall shape of the plot with the Brillouin plot for one fully isolated ion with $S = 1/2$ system with $g = 2.1$ (dash curve) indicates very slow magnetization which consistent with a weak antiferromagnetic interaction.

Taking into account the structure of **4** (Fig. 7), which consists of copper ions linked by double $\mu_{1,5}$ -dicyanamide groups in a 1D system, only one coupling parameter (J) was considered to interpret possible magnetic interactions in this compound (the interaction through the hydrogen bonding has not been considered). The experimental magnetic data have been fitted using the equation which was derived from the Bonner–Fisher [21] calculation based on the isotropic Heisenberg Hamiltonian: $H = -J\sum(S_i S_{i+1})$. The best fit parameters from 300 down to 2 K are found as $J = -5.1 \text{ cm}^{-1}$ and $g = 2.1$ with an error $R = 2.3 \times 10^{-5}$, where $R = \sum[(\chi_M T)_{\text{exp}} - (\chi_M T)_{\text{calc}}]^2 / \sum[(\chi_M T)_{\text{exp}}]^2$. The low superexchange parameter value found can be understood perfectly, if we consider the data reported in the literature. Indeed, the dicyanamide ligand in the coordination mode $\mu_{1,5}$ normally leads to a very weak antiferromagnetic coupling in Mn(II), Ni(II) or Cu(II) complexes and this interaction can even be zero or very weak ferromagnetic [22].

4. Conclusion

We have synthesized five new metal-organic frameworks including the first Cu(II) polymers with *para*- and *ortho*-ABN ligands. In these compounds *dca* and *para*-ABN ligands show the terminal as well as bridging bonding mode whereas *ortho*- and *meta*-ABN coordinated only in a monodentate fashion. The spin coupling constants, J , were estimated to be -2.35 and -5.1 cm^{-1} for **3** and **4**, respectively.

Acknowledgements

We acknowledge the financial support from the Council of Scientific and Industrial Research, New Delhi, India to Moumita Biswas. We also wish to acknowledge the use of the EPSRC's Chemical Database Service at Daresbury,

Cheshire, UK and grants given by the Ministerio de Educación y Ciencia (Programa Ramón y Cajal) and BQU2003/00539.

Appendix A. Supplementary data

Crystallographic data have been deposited at the Cambridge Crystallographic Data Centre with deposition numbers 602010–602014. These data can be obtained free of charge via <http://www.ccdc.cam.ac.uk/conts/retrieving.html> or from the Cambridge Crystallographic Data Centre, 12 Union Road, Cambridge CB2 IEZ, UK; fax: +44 1223 336 033; or e-mail deposit@ccdc.cam.ac.uk. Supplementary data associated with this article can be found, in the online version, at [doi:10.1016/j.poly.2006.08.008](https://doi.org/10.1016/j.poly.2006.08.008).

References

- [1] B. Moulton, M.J. Zaworotko, Chem. Rev. 101 (2001) 1629.
- [2] G.F. Swiegers, T.J. Malefetse, Chem. Rev. 100 (2000) 3483.
- [3] M.J. Zaworotko, Chem. Commun. (2001) 1.
- [4] T. Kuroda-Sowa, T. Horino, M. Yamamoto, Y. Ohno, M. Maekawa, M. Munakata, Inorg. Chem. 36 (1997) 6382.
- [5] K. Biradha, Y. Hongo, M. Fujita, Angew. Chem., Int. Ed. 39 (2000) 3843.
- [6] M.J. Zaworotko, Angew. Chem., Int. Ed. 39 (2000) 3052.
- [7] M. Fujita, Y.J. Kwon, S. Washizu, K. Ogura, J. Am. Chem. Soc. 116 (1994) 1151.
- [8] M. Fujita, K. Umemoto, M. Yoshizawa, N. Fujita, T. Kusukawa, K. Birdha, Chem. Commun. (2001) 509.
- [9] M. Eddaoudi, D.B. Moler, H. Li, B. Chen, T.M. Reineke, M. O'Keeffe, O.M. Yaghi, Acc. Chem. Res. 34 (2001) 319.
- [10] L.R. MacGillivray, S. Subramanian, M.J. Zaworotko, J. Chem. Soc., Chem. Commun. (1994) 1325.
- [11] (a) L.J. Moitsheki, S.A. Bourne, L.R. Nassimbeni, Acta Cryst. Sect. E. 61 (2005) m2580; (b) D. Vujovic, H.G. Raubenheimer, L.R. Nassimbeni, J. Chem. Soc., Dalton Trans. (2003) 631.
- [12] (a) D. Venkataraman, G.B. Gardner, S. Lee, J.S. Moore, J. Am. Chem. Soc. 117 (1995) 11600; (b) O.M. Yaghi, G. Li, H. Li, Nature 378 (1995) 703; (c) C.J. Kepert, M.J. Rosseinsky, Chem. Commun. (1999) 375.
- [13] (a) J.S. Miller, A.J. Epstein, Angew. Chem., Int. Ed. 33 (1994) 385; (b) M. Ohba, H. Okawa, Coord. Chem. Rev. 198 (2000) 313; (c) K.R. Dunbar, R.A. Heintz, Progr. Inorg. Chem. 45 (1997) 283; (d) E. Coronado, J.R. Galán-Mascaros, C.J. Gomez-Garcia, J. Ensling, P. Gutlich, Chem. Eur. J. 6 (2000) 552; (e) E. Coronado, M. Clemen-León, J.R. Galán-Mascaros, C. Giménez-Saiz, C.J. Gómez-García, E. Martínez-Ferrero, J. Chem. Soc., Dalton Trans. (2000) 3955.
- [14] S.R. Batten, K.S. Murray, Coord. Chem. Rev. 246 (2003) 103.
- [15] The United Kingdom Chemical Database Service D.A. Fletcher, R.F. McMeeking, D. Parkin, J. Chem. Inf. Comput. Sci. 36 (1996) 746.
- [16] (a) F.H. Allen, Acta Crystallogr. B58 (2002) 380; (b) I.J. Bruno, J.C. Cole, P.R. Edgington, M. Kessler, C.F. Macrae, P. McCabe, J. Pearson, R. Taylor, Acta Crystallogr. B58 (2002) 389.
- [17] G.M. Sheldrick, SHELXTL version 5.1, Bruker Inc., Madison, Wisconsin, USA, 1999.
- [18] Nonius COLLECT, DENZO, SCALEPACK, SORTAV: KapkaCCD B.V., Delft, The Netherlands, 1999.
- [19] G. Cascarano, A. Altomare, C. Giacovazzo, A. Guagliardi, A.G.G. Moliterni, D. Siliqi, M.C. Burla, G. Polidori, M. Camalli, Acta Crystallogr. A52 (1996) C-79.

- [20] D.J. Watkin, C.K. Prout, J.R. Carruthers, P.W. Betteridge, CRYSTAL Issue 11, Chemical Crystallography Laboratory, Oxford, UK, 1999.
- [21] O. Kahn, Molecular Magnetism, VCH, Weinheim, 1993, p. 252.
- [22] (a) J. Carranza, C. Brennan, J. Sletten, F. Lloret, M. Julve, J. Chem. Soc., Dalton Trans. (2002) 3164;
(b) J. Carranza, J. Sletten, F. Lloret, M. Julve, Inorg. Chim. Acta 357 (2004) 3304;
(c) J. Luo, M. Hong, J. Weng, Y. Zhao, R. Cao, Inorg. Chim. Acta 329 (2002) 59;
(d) A. Escuer, F.A. Mautner, N. Sanz, R. Vicente, Inorg. Chem. 39 (2000) 1668;
(e) R. Karmakar, C.R. Choudhury, D.L. Hughes, Glenn P.A. Yap, M.S. El Fallah, C. Desplanches, J.-P. Sutter, S. Mitra, Inorg. Chim. Acta 359 (2006) 1184.